

Conductive polymer composites and coated metals as alternative bipolar plate materials for all-vanadium redox-flow batteries

Burak Caglar^{1*}, Justin Richards², Peter Fischer¹, Jens Tuebke¹

¹Fraunhofer Institute for Chemical Technology (ICT) Applied Electrochemistry, Joseph-von-Fraunhofer str.7, 76327 Pfinztal, Germany

²Fraunhofer Institute for Chemical Technology (ICT) Applied Electrochemistry, Robert-Koch-Platz 8a, 38440 Wolfsburg, Germany

*Corresponding author. Tel: (+49) 7214640514; Fax: (+49) 7214640318; E-mail: burak.caglar@ict.fraunhofer.de

Received: 09 September 2013, Revised: 20 December 2013 and Accepted: 26 December 2013

ABSTRACT

In this study polypropylene (PP) based conductive composites and metal doped diamond like carbon (DLC) coated metallic substrates are studied as alternative bipolar materials for all-vanadium redox flow battery (VRFB). Graphite and carbon nanotube (CNT) filled PP based bipolar plates were produced via twin-screw co-rotating extruder and injection molding. Addition of 3 wt. % CNTs into highly filled graphite-PP matrix increased in-plane and through-plane electrical conductivities from 10 S/cm to 50 S/cm and from 2 S/cm to 10 S/cm respectively. PP composites with 78 wt. % graphite and 2 wt. % CNT filling ratio showed flexural strength value of 48,01 MPa. Produced bipolar plates were examined with galvanostatic charge-discharge test in a single-cell VRFB. Energy efficiency of 85,43 % at 25 mA/cm² and discharge power density of 78,48 mW/cm² at 75 mA/cm² were achieved and those values were found to be comparable with commercial bipolar plates. Titanium, vanadium, chromium and tungsten doped diamond-like coating (DLC) films were coated on metallic substrates (e.g. stainless steel 1.4301 and titanium alloy 3.7165) by a physical vapor deposition. The metallic dopant is necessary to achieve high conductivities in the order of ~100 S/cm. The values range from 0.5 to 35 S/cm for in-plane and from 10 to 110 S/cm for through-plane. The hydrogen evolution reaction (HER) and the anodic corrosion stability in 2 molar sulfuric acid constituted the main focus area for our investigations on metallic bipolar plates. An interesting material for coated metallic bipolar plate is the 10 μm Ti-DLC on 1.4301 which exhibits the highest hydrogen evolution overpotential of all investigated materials (710 mV μA/cm²). It also showed improved corrosion stability for anodic potentials. Copyright © 2014 VBRI press.

Keywords: Vanadium redox flow battery; polymer composites; metallic bipolar plates; diamond like carbon coating; Corrosion tests.



Burak Caglar is currently pursuing his Ph.D. and working as researcher in Fraunhofer ICT (Pfinztal), Germany. He obtained a B.S. in Chemical Engineering from Gazi University, Turkey in 2008. He received a M.S. in Nanoscience and Nanotechnology from University of Barcelona, Spain in 2010. He is currently working on the production of electrically conductive polymer composites and their applications as bipolar plates in all-vanadium redox flow batteries.



Justin Richards is currently pursuing his Ph.D. and working as researcher in Fraunhofer ICT (Wolfsburg), Germany. He obtained Diploma degree in Process Engineering -with the focus on plastics technology- from the University of Applied Sciences Ostfalia, Germany in 2008. His current research

interests include the production of metallic bipolar plates, corrosion protection/measurement of materials, and the development of coatings against corrosive mediums.

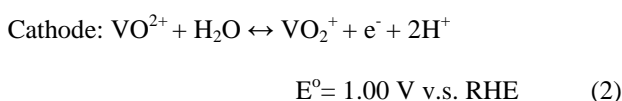
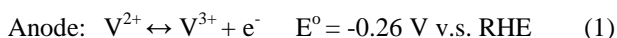


Peter Fischer is the head of Redox Flow Battery group in Fraunhofer ICT (Pfinztal), Germany since 2011. He obtained Ph.D. degree in Physical Chemistry from Heinrich-Heine-University Düsseldorf, Germany in 2011. His research interests are redox flow batteries, analytics and fuel cells.

Introduction

The limited future of fossil based energy sources and the increasing demand of electricity gave a rise to research and development of renewable energies. Photovoltaic facilities and wind turbines gained a considerable interest due to promising source of energy. However, they are environmentally friendly and cost efficient in long-run, fluctuations in the transmission of electricity is a severe disadvantage which has to be overcome with implementation of electrical energy storage systems at decentralized areas [1]. Redox flow batteries (RFB) are one of the storage systems with high energy efficiency, long working life and short response time. On the contrary to conventional batteries, in RFB, electrolyte is stored in external tanks and transferred to the battery core via pumps.

This design gives opportunity to independent power and energy capacity control [2]. When the energy capacity is determined with electrolyte concentration and volume of reservoirs [3], the system power can be tuned by changing electrode surface area and reaction rate of redox couples on the electrode surface by functionalizing with e.g. Iridium [4]. All-vanadium redox flow battery (VRFB) combines aforementioned advantages of redox flow batteries with the diversity of electrochemical characteristics of vanadium elements. VRFB converts electrochemical energy into electrical energy and vice-versa via redox reactions of vanadium electrolyte in two half-cells. Some sorts of redox flow batteries such as iron/chromium, iron/titanium and polysulfide bromine redox flow batteries suffer from electrolyte cross-contamination due to leakages or problems originate from membranes [5]. VRFB suppresses this issue due to usage of same electrolyte in both half-cells. The reactions between different valence states of vanadium during charging are as follows (Equation 1-2):



In VRFB (Fig. 1); electrolyte flow is controlled with flow-frames, ion balance was provided with proton exchange membrane (mostly ion-doped PTFE membranes), redox reactions take place on the surface of graphite felt electrode and produced electrons are transferred to the following cell or out of the battery with bipolar plates [6]. The standard electrolyte of VRFB is the solution of VOSO_4 in H_2SO_4 . This corrosive medium brings the necessity of chemical stability for each cell-component.

Bipolar plates (BPP) are one of the main cell components of VRFB. Besides, electron transfers, BPPs maintain the cell-integrity. Design and development of bipolar plates require characteristics like; high electrical conductivity, good mechanical stability, lower contact resistance especially with electrode, resistance against acidic medium and also a high overpotential for hydrogen evolution. Besides the material aspects they define about

60 % of the weight and about 30 % of the cost of one cell [7]. They also provide conduits for fluid flows of reactants and products of a cell. They remove heat from the active areas and carry the current from cell to cell. However, threshold values for bipolar plates was defined by Department of Energy, US [8], this standard is valid for fuel cell applications. If, redox flow battery cell-structure, electrolyte flow management and above-mentioned working principles of bipolar plates are considered; more precise evaluation of BPPs can be carried out with electrochemical analysis in VRFB medium such as corrosion measurement and cell-tests.

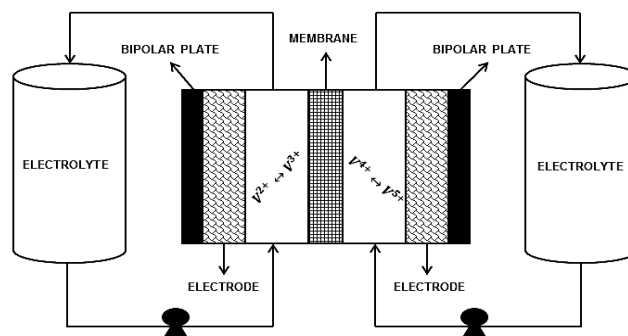


Fig. 1. Vanadium redox flow battery single cell; schematic.

Graphite was used as one of the main bipolar plate material due to its high electrical conductivity, low weight and good chemical stability [9]. Previously, parallel to the developments of fuel cell components; graphite plates are also used for redox flow batteries in the past. Graphite blocks were produced by sintering process and plates were machined to desired sizes. The main limitation of this method was the porosity of produced graphite plates. The porous structure was responsible of leakages and lower mechanical properties [10]. To overcome porosity disadvantage of graphite plates; carbon-carbon composites were developed. Their promising characteristics were; lower density and lower gas permeability compared to graphite plates. Besmann et al. produced carbon-carbon based bipolar plate by slurry-molding a chopped fiber preform and sealing this composite with chemical vapor infiltration (CVI). By CVI technique, methane was introduced at 1500 °C, and the deposition of carbon for hermetic structure was realized [11]. In another study, graphite and phenolic resin were mixed and compression molded. Instead of CVI process, carbonization method was used. After resin was converted to vitreous carbon at 1000 °C, to tighten up the structure and to increase electrical conductivity, composite was further heated up to 2100 °C and graphitization was performed [10]. However, high electrical properties and low weight of bipolar plates; the production of carbon-carbon composites were costly and requiring very long production cycles.

Conductive polymer composites (CPC) and coated-metallic bipolar plates are widely studied as alternative materials to conventional carbon-carbon plates. Polymer based BPPs use thermoplastics, thermosets or elastomers as matrix material and to ensure high electrical conductivities;

contain carbon-based conductive fillers like: graphite, carbon black, carbon fiber or carbon nanotubes [12]. These composites are produced via melt mixing (e.g. extruder, kneader) and injection or compression molding. They possess good corrosive behavior due to inert structure of polymer. Molding techniques shorten the production cycle-time, carry out porous-free bipolar plates and facilitate flow field design. As polymer itself behaves like insulating material, to convert it into conductive phase requires attentive introduction of conductive fillers into the matrix. The higher the concentration of filler, the higher the probabilities have to a porous structure or inferior mechanical properties. The dispersion state of filler is another important issue to take care. Especially high surface area fillers such as carbon nanotubes tend to create agglomerates due to inter-particle Van der Waals forces. To benefit from their properties, those agglomerates should be well disentangled and homogenous filler dispersion should be maintained [13].

As main issue in bipolar plate production is the high electrical conductivity, metallic bipolar plates are also regarded as promising alternative. The ease of manufacturing makes metallic substrates favorable over graphitic materials. Thin metallic plates can be easily shaped into any form useful for the application. Reducing the plate's thickness will result in a reduction of volume, mass and cost of a stack. Despite of their reduced thickness, metallic bipolar plates exhibit high ductility and strength in comparison to the graphite bipolar plates [14]. Unfortunately, their low stability against acidic solutions and the electrochemical characteristics of the metallic surface cover the main purpose of research. The corrosion of the metallic plates can result in a degradation of the membrane due to the affinity of the proton conducting groups in the membrane to adsorb the leached ions from the metal surface [15]. Furthermore protecting passive layers on the metallic bipolar plates, which might protect the surface against most corrosive attacks, usually tend to increase the electrical resistivity [16]. Metallic substrates such as precious metal coated stainless steels have been studied long for the application as bipolar plates in PEMFCs. The material compositions are not directly transferable from PEMFC to RFBs due to highly corrosive media in RFBs. The other crucial parameter for the development of bipolar plates in RFBs is the overpotential for hydrogen and oxygen evolution. To overcome the obstacle of corrosion in harsh environments, metallic plates have to be coated with organic or inorganic conductive layers by e.g. CVD- or PVD-processes [17, 18].

Since the first proposition of the diamond material to be used as electrochemical probes [19] in the 1980s, boron doped diamond (BDD) materials have been widely studied to be used for sensors and as probes which are operating in chemically aggressive and mechanically and thermally critical environments [20, 21]. There are several drawbacks, such as costs, producible area and quality, for the use of BDD for large scale electrodes. Therefore the research focused on diamond-like carbon coatings [22], which are deposited on relatively cheap metallic alloys. The carbon coatings [23] are doped with different metals to achieve the desired conductivity. In this study,

polypropylene based graphite and carbon nanotube filled conductive composites and metal doped DLC coated metallic substrates (1.4301 and 3.7165) were produced and electrically, mechanically and electrochemically tested as alternative bipolar plates for all-vanadium redox flow battery applications.

Experimental

Production of conductive polymer composite bipolar plates materials

Polypropylene (HL508FB) with melt flow rate (MFR) 800 was purchased from Borealis and used as matrix material. Synthetic graphite (KS5-75TT) from TIMCAL Graphite & Carbon was selected as primary conductive filler. Multi-wall carbon nanotubes (CNTs), with grade name: NC7000 (average diameter=9.5nm, average length=1.5µm, 90% carbon purity) from Nanocyl, Belgium was used as secondary filler. Montan wax (Licocene OP) (1-methyl-1,3-propanediyl ester) was received from Clariant.

Production method

Polymer matrix, conductive fillers and montan wax are melt mixed by means of Leistritz HP 27 x 52D co-rotating twin-screw extruder. To maintain better dispersion of CNTs, PP-CNT masterbatch (MB) with 15 wt.% CNT concentration is first prepared. In the second step; this masterbatch is diluted with graphite to obtain desired conductive filler concentration. Graphite and CNTs are introduced into PP matrix from side-feeders. The wax is added by dry mixing with CNT-PP masterbatch. Obtained granules are processed via Ferromatik Milacron K110/2K injection moulding machine to prepare bipolar plates. Production schema and process parameters are given in **Table 1** and **Table 2**. Injection speed and holding pressure are changed in a given window for each sample depending on filler concentration and final shape of product.

Table 1. Production scheme of polymer composite bipolar plates.

Samples	Polypropylene wt.%	Graphite wt.%	CNT wt.%	Wax wt.%
S-1	20	80	0	0
S-2	20	79	1	0
S-3	20	78	2	0
S-4	20	77	3	0
S-5	19	77	3	1
S-6	17	77	3	3

Table 2. Extruder and injection molding parameters for the production of polymer composite bipolar plates.

Extruder	Feedingzone	Zone 2-12	Zone 13-Die
Temperature Profile (°C)	180	210	240-250
Screw Speed (rpm)	1000 (CNT-PP Masterbatch)	300 (Graphite Addition)	
Injection Moulding	Feedingzone	Zone 1-3	Die
Temperature Profile (°C)	50	200-230	240
Injection Speed (cm ³ /s)	80-100		
Holding Pressure (bar)	900-1800		

Characterization of bipolar plates

Electrical conductivity of bipolar plates were measured both in through-plane and in-plane (bulk) directions. In-plane electrical conductivity was tested according to ISO 3915 standard method. Samples were cut into 70mm x 10 mm x 3mm size. Test setup for through-plane measurement (Fig. 2) was prepared with gold coated-copper plates (electrodes) which were protected by polyvinyl chloride (PVC) covers and samples were cut in the dimensions of 10mm x 10mm x 3mm. GDL paper (35 AA) from SGL Carbon was used to decrease the contact resistance between electrodes and bipolar plates. Both in through-plane and bulk conductivity measurements, current was applied by Keithley 2400 type sourcemeter and the voltage drop across the specimen was measured with Fluke 87V True RMS multimeter. To maintain good contact between bipolar plate and copper electrode, 1 MPa pressure was applied in through-plane measurements. By taking into account, polymer rich layer on the bipolar plates which was introduced during injection molding process, samples were grinded 0.1 mm from each side prior to through-plane electrical conductivity test.

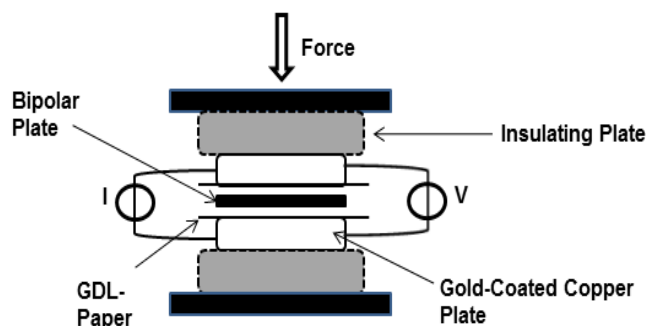


Fig. 2. Through-plane electrical conductivity setup.

To evaluate mechanical properties; prepared samples were tested according to ISO 178 three-point bending test and flexural strength values were measured. 2 mm/min flexural test speed was applied by Universal testing machine Inspekt Table 50KN (Hegewald & Peschke, Germany). The samples with dimensions of 60mm x 10mm x 3mm were conditioned at 23 °C and 50 % RH for 24 hours before testing. Supra 55 VP type field emission scanning electron microscopy (FE-SEM) from company ZEISS was used to show conductive particle dispersion inside the composite. Samples were prepared with liquid nitrogen and they were examined with high efficiency in-lens detector.

A single vanadium redox flow test-cell was constructed for the evaluation of produced bipolar plates in battery medium [12]. Samples were prepared in the dimensions of 85 mm x 60 mm x 3 mm and with 40 cm² active area. For galvanostatic charge-discharge test, constant current was applied from 1 to 4 ampere (A) by BaSyTec battery test software, obtained voltage was controlled within 0.8 V to 1.6 V and discharge power densities (mW/cm²) as well as

energy efficiency were calculated with following equations (3 to 5):

$$\text{Energy Efficiency \%} = (W_{\text{out}}/W_{\text{in}})*100 \quad (3)$$

$$W = \int U(t)*I(t)*dt \quad (4)$$

$$P_{\text{discharge}} = (1/t)\int U(t)*I(t)*dt \quad (5)$$

Production of coated metallic bipolar plates materials

Two different metallic substrates were chosen to be coated with a diamond like carbon film; a stainless steel alloy 1.4301 with a conductivity of 1.37*10⁴ S/cm and a titanium alloy 3.7165 with 5.85*10³ S/cm (Table 3).

Table 3. Metallic substrate materials.

American Iron and Steel Institute (AISI)	Material composition	Material number
304	X5CrNi18-10	1.4301
	TiAl6V4	3.7165

The protective coating on the metals consists of a carbon film doped with different transition metals to gain the desired conductivity [24]. The carbon coating is composed of sp² and sp³ hybridized carbon atoms [22] and the metals form carbide agglomerations in the coating [25].

Besides the increase in conductivity due to doping the DLC coatings the electrochemical behavior of the metals are also important for coatings in VRFB. Regarding the redox-reaction (Equation 1) taking place at around -255 mV vs. SHE, the crucial characteristic for the metallic dopant is its overpotential for hydrogen evolution. Although the metals do not exist in their pure state in their pure state in DLC coating Table 4 displays the chosen metals used in this project.

Table 4. Overpotential for hydrogen evolution of metallic dopants of their pure state for DLC in comparison to reference.

Metallic Dopant	Hydrogen evolution overpotential
Reference Graphite	-0.55 V [26]
Tungsten	-0.25 V [26]
Titanium	-0.63 V [28]
Chromium	-0.42 V [27]
Vanadium	-0.58 V [28]

Production method

The metallic substrates are cut from a rod with a 29 mm diameter into 5 mm thin chips. Then the samples are grinded and polished with diamond dispersion (3 μm). The polished chips are then mounted in a holder in a vacuum

chamber. The coating process is split in 4 different steps: Starting by cleaning the substrate with argon ion-etching. A metallic interlayer provides good adhesion between DLC coating and metallic substrate. The third step in the process is a gradient layer where the acetylene gas is fed to the reaction chamber until the desired ration of metallic dopant and carbon is reached. During the last phase the thickness is adjusted through the process duration. The characteristic parameter for the DLC coatings investigated in this project are 15% - 20 % metallic content and the coating thickness of 0.5 μm , 1 μm 2 μm , 3 μm , 5 μm and 10 μm .

Characterization of bipolar plates

For the corrosion measurements all Me-DLC coatings as well as the conductive polymer samples were treated after the following procedure: Prior to the measurement the samples were cleaned with isopropanol, rinsed with deionized water and dried in an air stream. The electrochemical tests of each sample starts with cathodic polarization for 5 min. Afterwards the OCV is taken for 30 min until it reaches steady state. A 3-electrode corrosion cell (

Fig. 3) filled with 100 ml 2 M H_2SO_4 provides the test environment for the material specimen. For the potentiodynamic measurement seen in **Fig. 1** the potential is varied with a sweep rate of 5 mV/s from OCV in cathodic direction until $-500 \mu\text{A}/\text{cm}^2$ is reached. Then the voltage is swept in anodic direction until a current of $500 \mu\text{A}/\text{cm}^2$ and back in cathodic direction until -300mV vs. OCV. For the comparison of different materials only the middle part of the current graph of the potential sweep is taken into account. The stability of the coating is analyzed by 200 cycles in potential range of -0.6V vs. NHE and 1.4V vs. NHE.

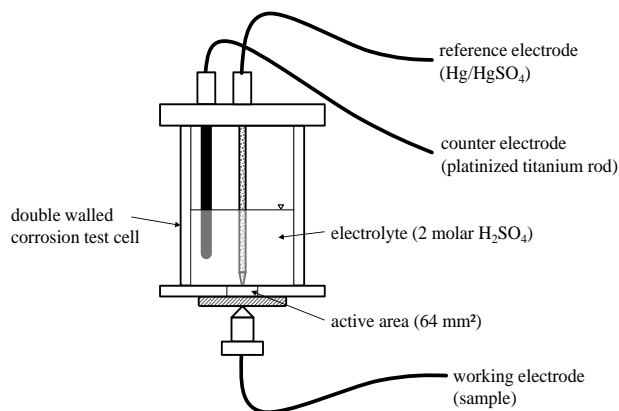


Fig. 3. Electrochemical schematic test setup.

Results and discussion

Conductive polymer composite bipolar plates electrical conductivity measurements

Electrical conductivity measurements (**Fig. 4**) showed that the substitution of 3 wt. % CNTs with the same amount of graphite increased the in-plane and through-plane electrical conductivities from 10 S/cm to 50 S/cm and from 2 S/cm to

10 S/cm respectively. The improvement in electrical conductivities can be attributed to decreased resistivity between graphite particles by introduction of highly conductive CNTs. Due to high aspect ratio, well-dispersed CNTs inside PP matrix behave as bridging filler between graphite particles [29].

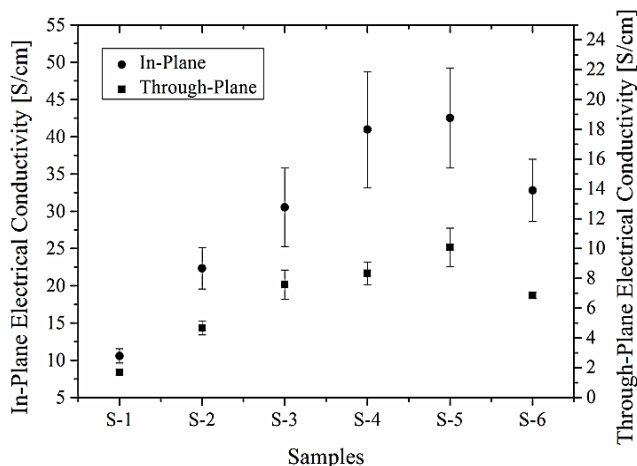


Fig. 4. In-plane and through-plane electrical conductivities of PP based bipolar plates.

This phenomenon was also visualized by FE-SEM pictures in **Fig. 5**. According to SEM pictures and improved electrical conductivity values, it can be concluded that relatively good dispersion of CNT was achieved. Preparation of CNT-PP masterbatch prior to addition of graphite in extruder step was found promising approach for better filler distribution.

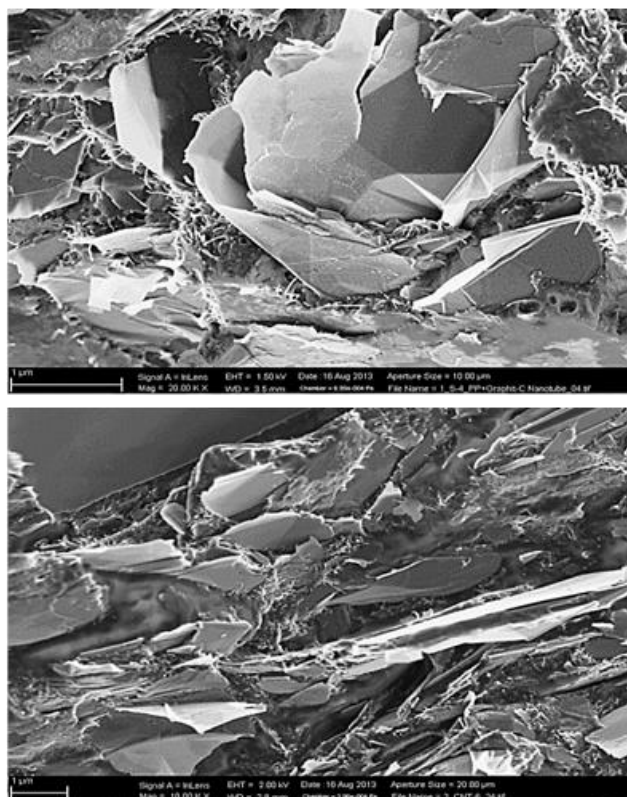


Fig. 5. FE-SEM pictures of S-4 sample (different part).

The production of highly filled thermoplastic composites is always challenging task in extruders and injection molding machines. Viscosity of composites increase by addition of fillers and after certain amount, polymer matrix loses its capability of wetting [30]. On the other hand, well-structured polymer-filler interphase also hinders the flow of composite. All these obstacles should be overcome to obtain porous free bipolar plates with desired electrical conductivity properties. To improve flow behavior of composite and to optimize filler dispersion; Montan wax was used as additive. Different concentrations were studied to understand its effect on electrical and mechanical properties. The additions of wax didn't bring any benefit to the electrical conductivity of bipolar plates. Nevertheless, final plate structure was improved. Especially, 3 wt. % wax added samples showed lower conductivity values at same total filler concentrations. However, addition of wax decreases overall viscosity of composite, at the same time, causes less shear stress which is applied by extruder components. The less the applied shear, the poor will be the filler dispersion and as a result; electrical conductivity tends to decrease.

Flexural strength measurement

Bipolar plates are important components for cell-integrity of the battery besides their electron transfer duty. Three point bending test creates similar mechanical stress that bipolar plates should withstand during test-cell preparation and upper-scale VRFB-applications. Proper filler dispersion and filler-matrix interaction are crucial for superior mechanical properties³¹. Especially, dispersion of CNTs plays a very critical role. However, CNTs are chosen due to their extraordinary mechanical strength, their agglomerates as well as pores in the composite structure behave as stress concentrations where materials are sensitive to breakage. Flexural strength results (Fig. 6) showed that CNT addition made positive contribution to the mechanical stability of bipolar plates.

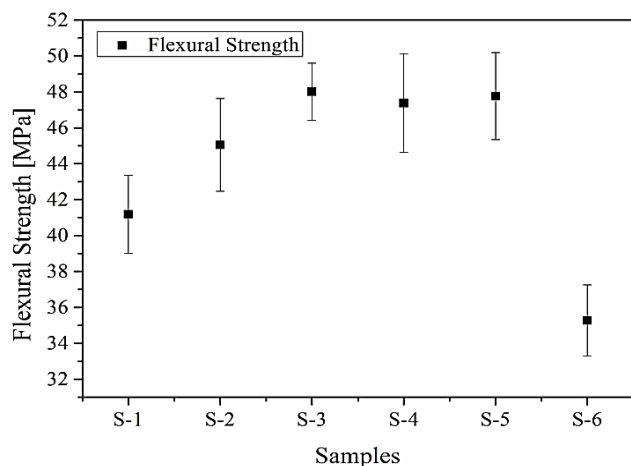


Fig. 6. Flexural strength values of PP based bipolar plates.

With 2 wt. % CNT substitution (S-3) flexural strength value increased from 41,19 to 48,01 MPa. Any further

improvement was achieved by increasing CNT content or adding 1 wt. % Montan wax. The dramatic decrease of sample S-6 (with 3 wt. % Montan wax) can be explained by very low viscosity and shorter polymer chains of Montan wax which causes to the brittleness of the composite. However, any standard for redox flow battery bipolar plates exist, according to Department of Energy, US⁸, minimum flexural strength value should be 25 MPa for fuel cell applications. In this aspect, produced bipolar plates fulfill mechanical strength requirements.

VRFB single-cell test

VRFB Single cell-test is an appropriate medium to test electrochemical behavior of composites and to evaluate potential of produced bipolar plates for further applications. Calculated energy efficiency and discharge power density values (equations 1-3) were compared with commercial grade Schunk bipolar plate (Fig. 7).

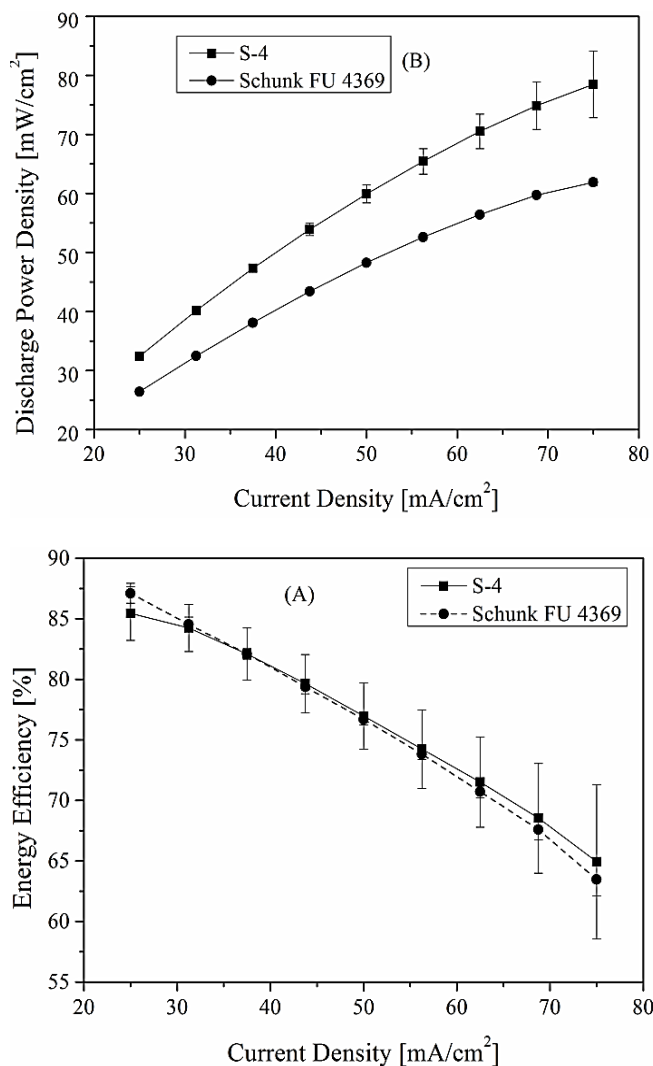


Fig. 7. VRFB Single cell-test. (A) energy efficiency v.s. current density (B) discharge power density v.s. current density.

Current density of 75 mA/cm² was achieved with produced bipolar plates and obtained energy efficiency

values were as good as commercial plate. This result shows the charge-discharge consistency of bipolar plates. Their capability of working at higher current densities is a sign for good electrical conductivity especially in through-plane direction. Superior discharge power density values (Fig. 7b) are indicators of favorable surface structure for vanadium redox reactions and increased reaction rates. As cell-tests were performed under same conditions and with same cell-components, main difference originates from bipolar plate itself. However, main redox reactions take place on graphite felt (electrode), BPPs are still responsible of a part of those reactions. It can be concluded that surface grinding of conductive polymer composites and higher surface area of CNTs create more possibility for the conversion of vanadium species on the surface of produced bipolar plates.

Coated metallic bipolar plates microscopic results

Fig. 8 shows a SEM cross-section of a W-DLC coating. As explained in the production part of this paper the interlayer as well as the gradient layer and the final top-layer can be easily identified. The microscopic picture shows a relatively rough surface.

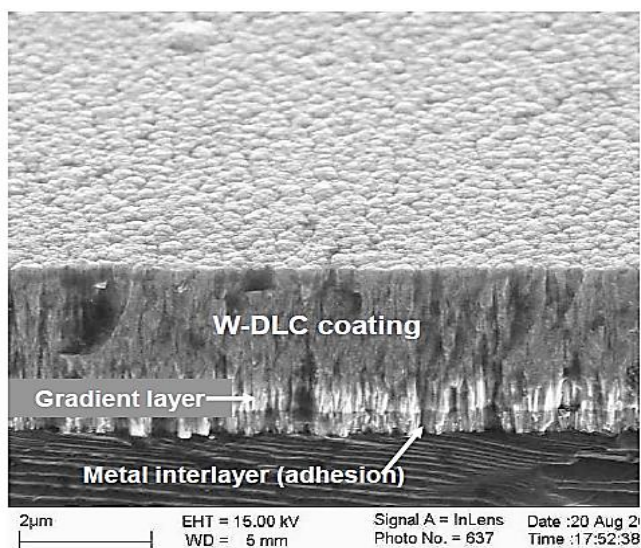


Fig. 8. SEM cross section of W-DLC coating (with courtesy of Fraunhofer IST Braunschweig).

Although no actual pores can be seen in the SEM-cross section, the microscopic image in Fig. 9a (recorded with a Keyence with a VHX-600) certainly states that there are several indentations in the top-layer of the specimen. These pinholes most certainly are the point of corrosion attack due to electrochemical potential and harsh environment (2 M sulfuric acid). The degradation and also delamination of the coating is displayed in Fig. 9b). The elevation in the middle of the corrosion pit was also noticed for other Ti-DLC coatings e.g. 10 µm Ti-DLC see Fig. 10.

After galvanostatic tests in 2 M sulfuric acid the specimen also exhibited defects in the coating. The degradation of the cathodic load (Fig. 11 a) does not result from an actual corrosion process but rather from hydrogen produced on the metallic interlayer or substrate resulting in

a delamination of parts of the coating. In comparison to the anodic load (Fig. 11b) where corrosion pits are visible, the roughness of the specimen which was investigated under cathodic load displayed a relatively smooth and shiny corrosion base.

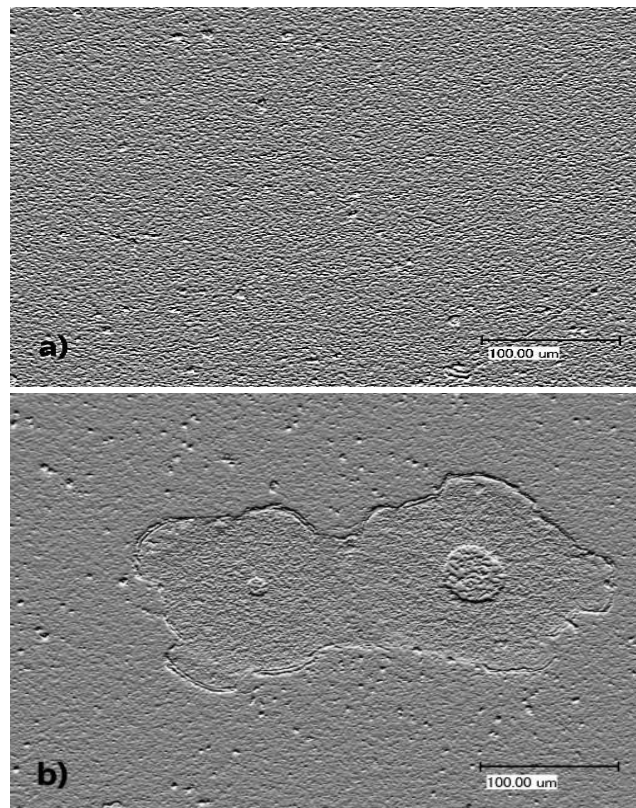


Fig. 9. (a) before and (b) after electrochemical stability-test for 200 cycles of a 3 µm Ti-DLC on 1.4301.

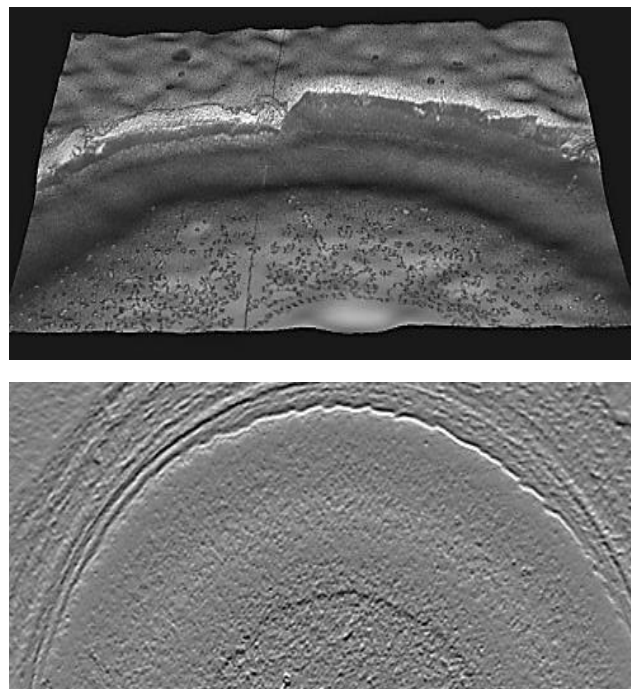


Fig. 10. Microscopic images of 10 µm Ti-DLC on 1.4301 after 200 cycle electrochemical stability test in 2 M sulfuric acid; Top 3D image of the defect seen in the bottom.

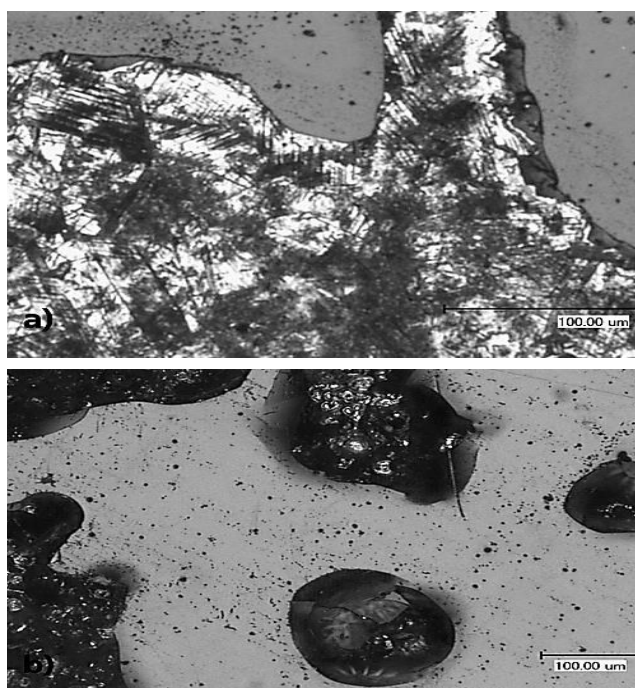


Fig. 11. Microscopic images of 3 μm Ti-DLC on 1.4301 after constant current for 80h; top: galvanostatic load at $-250 \mu\text{A}/\text{cm}^2$ and bottom: galvanostatic load at $+250 \mu\text{A}/\text{cm}^2$.

Electrochemical results

The results concerning the electrochemical behavior of the coating thickness of a metal doped DLC (here: Ti-DLC) is displayed in **Fig. 12**. Besides the higher corrosion currents in the anodic potential range of the thicknesses 0.5 and 1 μm the hydrogen evolution starts also earlier. The most promising coating material, considering the electrochemical behavior of one cycle in 2 molar sulfuric acid, is Ti-DLC with a thickness of 5 and 10 μm . Regarding the corrosion stability of 200 cycles 10 μm coating thickness of Ti-DLC exhibits just little degradation of the coating.

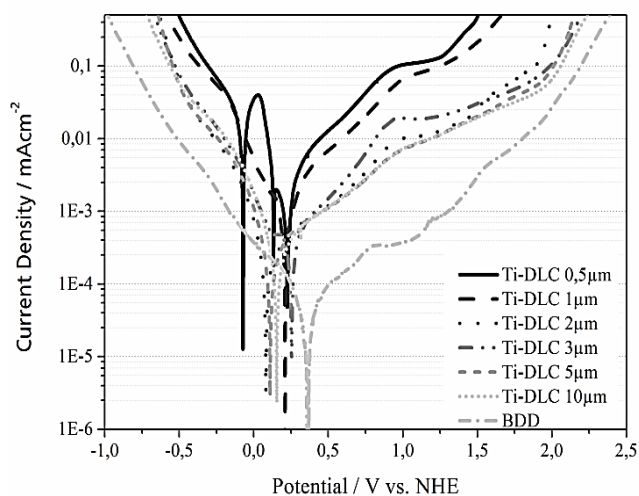


Fig. 12. Potentiodynamic measurements Me-DLC for one cycle $dU/dt = 5 \text{ mV/s}$, $|i_{\text{max}}| = 500 \mu\text{A}/\text{cm}^2$.

Nevertheless the thickness of a coating does not necessarily correlates with its electrochemical stability. For example the 3 μm corrodes faster than the 2 μm Ti-DLC sample (**Fig. 13**). Therefore another effect like pinhole distribution and size must be part of the degradation of the coatings on the metallic substrates.

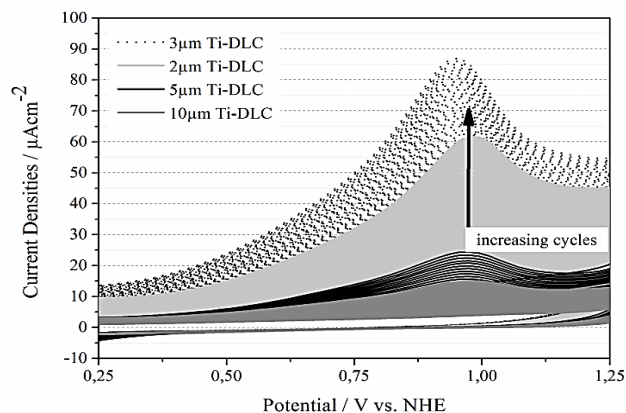


Fig. 13. A characteristic anodic section of 200 cycles electrochemical stability test.

The electrochemical behavior of the coatings on the different substrates is very similar (**Fig. 14**). However the dopant material which has the highest overpotential for hydrogen evolution is titanium doped DLCs, it provides an acceptable corrosion stability in the anodic potential range. V-DLC coatings show slightly lower hydrogen overpotentials but they also display lower current for the oxide formation at 1.1 V vs. on the anodic branch.

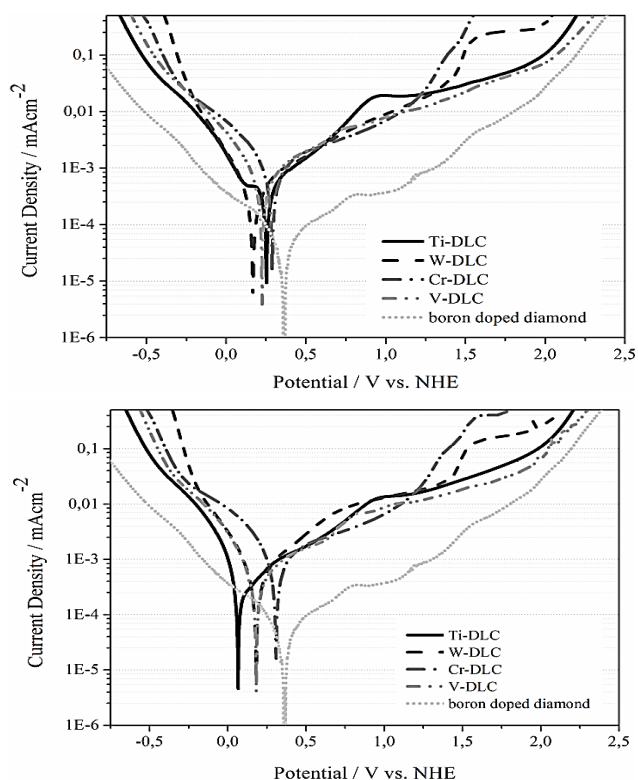


Fig. 14. Potentiodynamic measurements of 3 μm Me-DLC coatings on the top: 1.4301 and bottom: 3.7165; $dU/dt = 5 \text{ mV/s}$, $|i_{\text{max}}| = 500 \mu\text{A}/\text{cm}^2$.

Regarding the electrochemical behavior of different refractory metals as dopant in comparison to their pure state (**Table 4**) the metals consisting as carbids in the DLC coatings exhibit similar hydrogen evolution overpotentials. Although there are differences for the different coating thicknesses (0.5 μm lowest value and respectively 10 μm the highest value). The comparison of the electrochemical test results of the metal doped DLC with the reference materials (graphite and boron doped diamond) and also with the S4 sample of the conductive polymer composite sample is displayed in **Fig. 15** and **Table 5**. The corrosion stability of S4 for anodic potentials is almost as good as the boron doped diamond. The hydrogen evolution of the S4 is also equally good as the reference graphite material. Considering the oxygen evolution the Ti-DLC coating exhibits a higher overpotential compared to the graphite and S4 material.

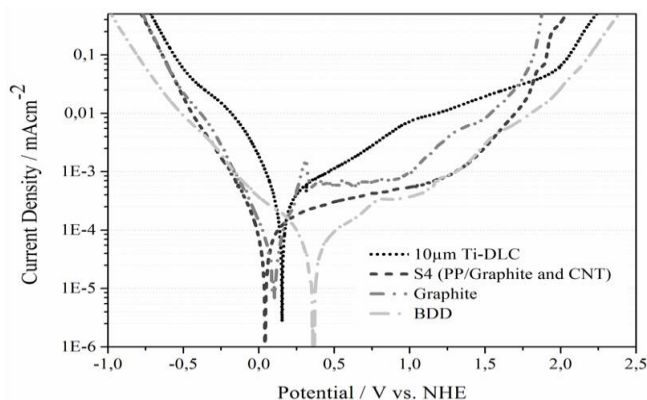


Fig. 15. Potentiodynamic measurements 10 μm Ti-DLC, reference material and PP/Graphite and CNT; $dU/dt = 5 \text{ mV/s}$, $|i_{\text{max}}| = 500 \mu\text{A/cm}^2$.

Table 5. Overpotentials for hydrogen and oxygen evolution of the electrochemical tested materials in comparison to reference graphite and CVD-Diamond.

Material	Potentials vs. NHE ¹		
	Hydrogen evolution	Oxygen evolution	
Ref.	Graphite	-0.65	1.80
	BDD	-0.80	2.20
	PP/C+CNT	-0.60...-0.45	1.70...1.75
Dopant for DLC coatings on 3.1765	Ti	-0.57...-0.51	1.85...2.00
	V	-0.55...-0.45	2.00...2.20 ²
	Cr	-0.40...-0.37	1.35...1.40
	W	-0.31...2.55	1.45...1.65
Dopant for DLC coatings on 1.4301	Ti	-0.65...-0.60	1.90...2.05
	V	-0.45...-0.35	2.05...2.15 ²
	Cr	-0.40...-0.37	1.35...1.40
	W	-0.30...-0.28	1.45...1.50

¹Potentials at -0.1 mA/cm^2 with a sweep rate of 5 mV/s in 2 molar sulfuric acid. ²On many samples severe pitting corrosion was detected.

Conclusion

Alternative bipolar plates for the application of VRFB were extensively studied. Conductive composite bipolar plates were produced via extruder and injection molding which give a chance for time and cost effective production cycles and co-production of cell components. Metallic substrates coated via PVD process with a metal doped DLC possess a great possibility for an alternative bipolar plate material. The conductivity, mechanical stability and high overpotentials for the crucial hydrogen evolution are positive aspects for their usage. Nevertheless the coating stability needs to improve in using metal bipolar plates in VRFBs. Carbon nanotubes were found as promising secondary filler to achieve high electrical conductivities in both through-plane and in-plane directions. All produced plates showed good mechanical stability and optimized CNT concentration increased flexural strength value. Montan wax didn't made any significant benefit to electrical and mechanical properties of bipolar plates. Nevertheless the application of wax made the addition of high amount of conductive fillers easier and improved flow behavior of composite melt. Higher energy efficiencies and discharge power densities were showed that produced composites have potential to be used in VRFB. The titanium as a metal dopant proved itself as a good enhancement for the electrochemical behavior in 2 molar sulfuric acid. The vanadium, chromium and tungsten all displayed lower overpotentials for the hydrogen evolution. The corrosion stability over 200 cycles was best achieved through a 10 μm Ti-DLC coating on 1.4301. The most crucial aspect is the porosity or pinhole distribution in the DLC coatings. Metal doped diamond coated metallic substrates and extrinsically conductive polymer bipolar plates should be examined with long-term cell-tests for further information about its electrochemical stability in realistic conditions.

Acknowledgements

The research work of polymer composite bipolar plates has received funding from the European Community's Seventh Framework Programme (FP7/2007-2013) under grant agreement no. 238363. We also acknowledge the financial support of this work by the Fraunhofer MEF Project founding.

Reference

- Flox, C. *et al. Applied Energy* **2013**, 109, 344–351
DOI: [10.1016/j.apenergy.2013.02.001](https://doi.org/10.1016/j.apenergy.2013.02.001)
- Li, L. *et al. Advanced Energy Materials* **2011**, 1, 394–400
DOI: [10.1002/aenm.201100008](https://doi.org/10.1002/aenm.201100008)
- Gattrell, M. *et al. Journal of the Electrochemical Society* **2004**, 151, A123-A130
DOI: [10.1149/1.1630594](https://doi.org/10.1149/1.1630594)
- Wang, W.H.; Wang, X.D. *Electrochimica Acta* **2007**, 52, 6755–6762
DOI: [10.1016/j.electacta.2007.04.121](https://doi.org/10.1016/j.electacta.2007.04.121)
- Prifti, H. *et al. Membranes* **2012**, 2, 275-306
DOI: [10.3390/membranes2020275](https://doi.org/10.3390/membranes2020275)
- Rahman, F.; Skyllas-Kazacos, M. *Journal of Power Sources* **2009**, 189, 1212–1219
DOI: [10.1016/j.jpowsour.2008.12.113](https://doi.org/10.1016/j.jpowsour.2008.12.113)
- Li, X.; Sabir, I. *International Journal of Hydrogen Energy* **2005**, 30, 359-371
DOI: [10.1016/j.ijhydene.2004.09.019](https://doi.org/10.1016/j.ijhydene.2004.09.019)
- Liao, S.H. *et al. Journal of Power Sources* **2008**, 185, 1225–1232
DOI: [10.1016/j.jpowsour.2008.06.097](https://doi.org/10.1016/j.jpowsour.2008.06.097)
- Yuan, X.Z.; Wang, H.; Zhang, J.; Wilkinson, D.P. *Journal of New Materials for Electrochemical Systems*, **2005**, 8, 257-267

10. Cunningham, B.D.; Huang, J.; Baird, D.G. *International Materials Reviews*, **2007**, 52, 1
DOI: [10.1179/174328006X102556](https://doi.org/10.1179/174328006X102556)
11. Besmann, T.M. et al. *Materials Research Society Symposium Proceedings*, **2003**, 756, FF7.1.1.
12. Antunes, R.A.; de Oliveira, C.L.M.; Ett, G.; Ett, V. *Journal of Power Sources*, 2011, 196, 2945-2961
DOI: [10.1016/j.jpowsour.2010.12.041](https://doi.org/10.1016/j.jpowsour.2010.12.041)
13. Liao, S.H. et al. *Journal of Power Sources* **2008**, 176, 175-182
DOI: [10.1016/j.jpowsour.2007.10.064](https://doi.org/10.1016/j.jpowsour.2007.10.064)
14. Lee, N. J. et al. *Bulletin of the Korean Chemical Society*, **2012**, 33, 3589-3593
DOI: [10.5012/bkcs.2012.33.11.3589](https://doi.org/10.5012/bkcs.2012.33.11.3589)
15. Trappmann, C. Metallische Bipolarplatten für Direkt-Methanol Brennstoffzellen, *Cuvillier*, **2010**, ISBN: 9783869555478
16. Antunes, R. A. et al. *International Journal of Hydrogen Energy*, **2010**, 35, 3632-3647
DOI: [10.1016/j.ijhydene.2010.01.059](https://doi.org/10.1016/j.ijhydene.2010.01.059)
17. Lee, S.J.; Huang, C.H.; Chen, Y.P. *Journal of Materials Processing Technology*, **2003**, 140/1-3, 688-693.
DOI: [10.1016/S0924-0136\(03\)00743-X](https://doi.org/10.1016/S0924-0136(03)00743-X)
18. Wind, J.; Späh, R.; Kaiser, W.; Böhm, G. *Journal of Power Sources*, **2002**, 105/2, 256-260.
DOI: [10.1016/S0378-7753\(01\)00950-8](https://doi.org/10.1016/S0378-7753(01)00950-8)
19. Terranova, M. L. *Diamond and Related Materials* **2001**, 10, 627-630
DOI: [10.1016/S0925-9635\(00\)00435-0](https://doi.org/10.1016/S0925-9635(00)00435-0)
20. Klages, C.P. *Applied Physics* **1993**, A56, 513-526
21. Angus, J.C., Hayman, C.C. *Science*, **1988**, 241, 913-921
DOI: [10.1126/science.241.4868.913](https://doi.org/10.1126/science.241.4868.913)
22. Angus, J.C. *Annual Review of Materials Science*, 21 (1991) 221-248
DOI: [10.1146/annurev.ms.21.080191.001253](https://doi.org/10.1146/annurev.ms.21.080191.001253)
23. Noack, J.; Tuebke, J. *ECS Transactions* **2010**, 25, 235-245
DOI: [10.1149/1.3414022](https://doi.org/10.1149/1.3414022)
24. Tsay, Y.F. *Journal of Applied Physics*, **1972**, 43, 3677-3682
DOI: [10.1063/1.1661788](https://doi.org/10.1063/1.1661788)
25. Mabuchi, Y. *Tribology International* **2013**, 62, 130-140
DOI: [10.1016/j.triboint.2013.02.007](https://doi.org/10.1016/j.triboint.2013.02.007)
26. Vetter, K.J. *Elektrochemische Kinetik*, Springer-Verlag, Berlin-Göttingen-Heidelberg, **1961**, 432
DOI: [10.1002/bbpc.19620660214](https://doi.org/10.1002/bbpc.19620660214)
27. Rüetschi, P. *The Journal of Chemical Physics*, **1955**, 23, 195-199
DOI: [10.1063/1.1740527](https://doi.org/10.1063/1.1740527)
28. Ezaki, H. *Electrochimica Acta*, **1993**, 38, 557-564
DOI: [10.1016/0013-4686\(93\)85012-N](https://doi.org/10.1016/0013-4686(93)85012-N)
29. Dhakate, S.R.; Sharma, S.; Chauhan, N.; Seth, R.K.; Mathur R.B. *International Journal of Hydrogen Energy*, **2010**, 35, 4195-4200
DOI: [10.1016/j.ijhydene.2010.02.072](https://doi.org/10.1016/j.ijhydene.2010.02.072)
30. Yeetsorn R. Development of Electrically Conductive Thermoplastic Composites for Bipolar Plate Application in Polymer Electrolyte Membrane Fuel Cell. Ontario, Canada. University of Waterloo. PhD. Thesis, **2010**.
31. Lafdi, K.; Fox, W.; Matzek, M.; Yildiz, E. *Journal of Nanomaterials*, **2008**, 3, 1-8
DOI: [10.1155/2008/310126](https://doi.org/10.1155/2008/310126)

Advanced Materials Letters

Publish your article in this journal

ADVANCED MATERIALS Letters is an international journal published quarterly. The journal is intended to provide top-quality peer-reviewed research papers in the fascinating field of materials science particularly in the area of structure, synthesis and processing, characterization, advanced-state properties, and applications of materials. All articles are indexed on various databases including [DOAJ](https://doi.org/10.1016/j.ijhydene.2010.01.059) and are available for download for free. The manuscript management system is completely electronic and has fast and fair peer-review process. The journal includes review articles, research articles, notes, letter to editor and short communications.

